Stereochemical Probes of Bovine Plasma Amine Oxidase: Evidence for Mirror Image Processing and a Syn Abstraction of Hydrogens from C-1 and C-2 of Dopamine†

Martin F. Farnum and Judith Pollock Klinman*
Department of Chemistry, University of California, Berkeley, California 94720
Received January 17, 1986; Revised Manuscript Received June 3, 1986

ABSTRACT: Bovine plasma amine oxidase (PAO) has previously been shown to catalyze a nonstereospecific loss of tritium from [2(*R*)-^{3}H]- and [2(*S*)-^{3}H]dopamines, attributed to multiple, catalytically active binding sites for substrate [Summers, M. C., Markovic, R., & Klinman, J. P. (1979) *Biochemistry 18*, 1969–1979]. Analysis of products formed from incubation of dopamine with PAO in tritiated water indicates a stereospecific, *pro-R*, incorporation of label at C-2. Thus, tritium washout (random) and washin (*pro-R*) are not the microscopic reverse of one another. We conclude that the (enamine) intermediates leading to tritium washin are nonequivalently bound. The observation of *pro-R* incorporation has provided a straightforward synthetic route to [1(*R*)-^{2}H,2(*R*)-^{3}H]- and [1(*S*)-^{2}H,2(*R*)-^{3}H]dopamines, which upon oxidation with PAO are expected to be processed preferentially by 1*S* and 1*R* cleavage, respectively. From previously measured isotope effects, we predict the loss of tritium from the 1(*R*)-^{2}H and 1(*S*)-^{2}H samples to be 74:8 for a syn relationship between cleavage at C-1 and C-2 vs. 21:90 for an anti relationship. The observation of a 68:18 ratio at 100% conversion provides strong evidence for a syn cleavage. The data support a mechanism in which a single base catalyzes a 1,3-prototrophic shift of hydrogen from C-1 of the substrate to cofactor, followed by exchange from C-2. Additionally, the results confirm the presence of alternate binding modes for dopamine at the active site of bovine plasma amine oxidase. This interaction of dopamine with plasma amine oxidase is a rare example of mirror-image catalysis in which a *single* substrate has two functional binding orientations on an enzyme surface.

Copper-containing amine oxidases catalyze the oxidative deamination of primary amines. Substrate oxidation occurs in an anaerobic process to produce enzyme-bound imine (Palcic & Klinman, 1983), which upon hydrolysis yields product aldehyde, eq 1. In a subsequent step, dioxygen reacts with

$$E_{ox} + RCH_2NH_3^+ \underset{k_2}{\overset{k_1}{\rightleftharpoons}} E_{red-^+NH=CHR} \xrightarrow{k_3} E_{red-NH_2}(RCHO) \quad (1)$$

reduced enzyme to generate hydrogen peroxide and free enzyme, eq 2. We have retained aldehyde in eq 2, since it is

$$E_{red-NH_2}(RCHO) + O_2 \xrightarrow{k_5} E_{ox} + RCHO + NH_4^+ + H_2O_2 \quad (2)$$

not yet clear whether product release precedes enzyme reoxidation. Additionally, controversy exists regarding the point of ammonia release. As illustrated in eq 1, ammonia undergoes transfer from substrate to an enzyme-bound cofactor in the course of enzyme reduction. This mechanism is consistent with reports that pyrroloquinoline quinone functions as cofactor for plasma amine oxidase (Lobensteen-Verbeek et al., 1984; Ameyama et al., 1984) and the finding that the rate of ammonia release is oxygen-dependent for plasma enzyme from pig (Rius et al., 1984). It should be noted, however, that an earlier study by Abeles and co-workers (Suva & Abeles, 1978) on the bovine enzyme indicated a stoichiometric burst of ammonia release under anaerobic conditions.

With the recent evidence in support of pyrroloquinoline quinone, major unanswered questions exist for bovine plasma amine oxidase. These include the direct demonstration of a role for cofactor in substrate binding and activation, the characterization of copper catalysis (i.e., does copper interact with cofactor and/or substrate or is its role restricted to oxygen activation), and the determination of active site residues participating in catalysis [cf. Farnum et al. (1986)]. In addition, the origin of mirror-image catalysis, proposed for the phenethylamine derivative dopamine (Summers et al., 1979), and the relationship of this property to topologic constraints at the enzyme active site remain to be elucidated.

It has previously been shown that the stereochemical path of bovine plasma amine oxidase is substrate-dependent. In the case of benzylamine, oxidation entails exclusive abstraction of the *pro-S* hydrogen at C-1 (Battersby et al., 1979), analogous to the reaction catalyzed by pea seedling amine oxidase (Battersby et al., 1976). By contrast, Summers et al. (1979) reported a nonstereospecific loss of hydrogen from both C-1 and C-2 of dopamine. This lack of specificity has been proposed to be "apparent" and to be a consequence of alternate substrate binding modes characterized by opposing but absolute stereochemistries. Unexpectedly, large differences in primary isotope effects were detected for the oxidation of [1(*S*)-^{3}H]- and [1(*R*)-^{3}H]dopamines, $^T(V/K)$ = 25–30 and 4–6, respectively (Summers et al., 1979).

In this study, we have utilized this large differential in isotope effect to constrain dopamine to be oxidized preferentially via a single binding mode. Through a combination of enzymatic and chemical synthetic steps, dopamine samples that are both chirally tritiated at C-2 and chirally deuterated at C-1 have been prepared. Analysis of tritium release to solvent from these samples in the course of bovine plasma amine oxidase catalysis provides direct evidence, first, in support of mirror-image catalysis and, second, that the C–H bond

† Supported by a grant from the NSF (PCM-83-16118).
* Author to whom correspondence should be addressed.

0006-2960/86/0425-6028$01.50/0

cleavages at C-1 and C-2 occur in a syn manner. Overall, the results presented herein have important implications regarding possible substrate–cofactor interactions and provide a working model for the bovine plasma amine active site.

Experimental Procedures

Materials

Dopamine was obtained from Sigma, NAD^+ and NADH were from P-L Biochemicals, and [$^2H_6$]ethyl alcohol and DL-[2-^{2}H]dihydroxyphenylalanine (DL-[2-^{2}H]Dopa) were purchased from Merck Isotopes. Tritiated water (Amersham) was diluted to final specific activities of 2.3×10^6 and 8.7×10^6 cpm/μmol from a stock at specific activity of 5 Ci/mL. All organic reagents were obtained from either Aldrich or Sigma. Dry tetrahydrofuran was prepared by refluxing over Na/benzophenone. Methanol was heated over Mg turnings to remove residual water.

Liver and yeast alcohol dehydrogenases came from Sigma, while catalase was purchased from Boehringer. Bovine plasma amine oxidase was purified by modification of the procedure of Yamada and Yasunobu (1962). Tyrosine decarboxylase from *Streptococcus forcalis* type I was purchased from Sigma as a crude acetone extract.

Methods

High-performance liquid chromatography (HPLC) analyses were performed on a Beckman gradient liquid chromatographic system model. Product elution was followed by monitoring absorbance at 280 nm on a Hitachi variable-wavelength detector. Radioactivity was determined by liquid scintillation on a Beckman 8000 instrument. The 90-MHz ^{1}H NMR spectra were recorded on a Varian EM390 spectrometer in $CDCl_3$ or D_2O where appropriate. Computer graphics drawings of enzyme intermediates were generated with the FORTRAN program VIEW developed by Thomas Pollard at the University of California, Berkeley. VIEW, an upgraded version of SPACEFIL (Henry, 1983) featuring a command-style user interface, was run on a LSI-11 computer fitted with a Tektronix 4025A display. Initial *xyz* coordinates were obtained from crystallographic data for methoxatin (Cruse, 1980) and dopamine hydrochloride (Bergin, 1968). All structures reflect our attempts to minimize nonbonding interactions while giving attention to mechanistic constraints as stated in the text.

Enzymatic Preparation of [2(R)-^{3}H]-2-(3,4-Dihydroxyphenyl)ethyl Alcohol. Protonated dopamine (15 μmol) was incubated with plasma amine oxidase (0.3 unit of 0.24 unit/mg), catalase (0.3 mg of 39 000 units/mg), liver alcohol dehydrogenase (3.0 units of 1.6 units/mg), NADH (1.1 μmol), cyclohexanol (15 μmol), and 100 μmol of sodium potassium phosphate, pH 7.0, in a total volume of 1.0 mL of tritiated water, final specific activity = 2.3×10^5 cpm/μmol. After 8.5 h, the tritiated water was removed from the reaction by bulb-to-bulb lyophilization of the frozen reaction mixture. Residual tritiated water was removed by rinsing the residue with 6 1.0-mL portions of 0.001 N HCl. The residue was dissolved in 1.0 mL of 0.001 N HCl and deproteinized by centrifugation through an Amicon micropartition membrane. The reaction mixture was then injected onto an Altex ODS Ultrasphere, semipreparative reverse-phase HPLC column (1.0 × 25 cm) preequilibrated with an isocratic mixture of 95% methanol and 5% acetic acid (1%). The column was run at a flow rate of 3.5 mL/min. Purified [2-^{3}H]-2-(3,4-dihydroxyphenyl)ethyl alcohol, *ca.* 6.6 μmol, with specific activity of 2.0×10^5 cpm/μmol was diluted with unlabeled alcohol to give 1 mmol of product with a final specific activity of 1290 cpm/μmol.

Synthesis of [1(S)-^{2}H]Dopamine from DL-[*2-^{2}H]Dopa.* [1(*S*)-^{2}H]Dopamine was synthesized by enzymatic decarboxylation of a DL mixture of [2-^{2}H]Dopa employing tyrosine decarboxylase. A total of 100 μmol (28 mg) of the hydrobromide of DL-[1-^{2}H]Dopa was added to 10 mL of 0.064 M sodium acetate buffer previously degassed and equilibrated with argon. Following incubation at 37 °C for 30 min, 22 mg of tyrosine decarboxylase (0.4–0.5 unit/mg) was added to initiate the reaction. Dopamine production was monitored by analytical reverse-phase HPLC. Typically, a 50-μL aliquot of the reaction mixture was added to 200 μL of a 95% acetic acid (1%)–5% methanol mixture, filtered through an Amicon ultrafiltration membrane to remove the protein, and injected (50 μL) onto an C-18 analytical reverse-phase column. Elution was effected with an isocratic mobile phase, 95% acetic acid (1%)–5% methanol, at a flow rate of 1.0 mL/min. An excellent separation of Dopa and dopamine was obtained under these conditions with retention times of 8.0 and 14.0 min, respectively.

The reaction appeared to be 95% complete after 5 h. Subsequent large-scale purification of the product [1(*S*)-^{2}H]dopamine from enzymatically inactive D-Dopa required different HPLC conditions. Good resolution was achieved by using 1.0-mL injections onto an Altex semipreparative reverse-phase column with a mobile phase consisting of 70% acetic acid (1%)–30% methanol. Dopamine fractions were pooled, the solvent was evaporated in vacuo, and samples were stored frozen under nitrogen gas to avoid air oxidation.

Enzymatic Preparation of [1(S)-^{2}H,2(R)-^{3}H]-2-(3,4-Dihydroxyphenyl)ethyl Alcohol. Conditions used for the enzymatic oxidative deamination of [1(*S*)-^{2}H]dopamine were similar to those described earlier for protonated dopamine, with the exception that the tritiated water had a specific activity = 3.6×10^6 cpm/μmol.

Following removal of tritiated water and deproteinization, [1(*S*)-^{2}H,2(*R*)-^{3}H]-2-(3,4-dihydroxyphenyl)ethyl alcohol was purified from the reaction mixture by semipreparative reverse-phase HPLC. A mobile phase of 85% acetic acid (1%)–15% methanol was used, at a flow rate of 3.5 mL/min. From a single 1.0–mL injection, 3.5 μmol of tritiated product with specific activity = 3.6×10^6 cpm/μmol was collected and diluted to 1 mmol with unlabeled 2-(3,4-dihydroxyphenyl)ethyl alcohol. The residue obtained upon solvent evaporation in vacuo was stored overnight in a vacuum desiccator containing P_2O_5.

Preparation of [4(R)-^{2}H]NADH. [4(*R*)-^{2}H]NADH preparation followed the method of Rafter and Colowick (1957). Yeast alcohol dehydrogenase (65 units) was incubated with 200 mg of NAD^+ and 0.71 mL of [$^2H_6$]ethyl alcohol in 20 mL of tris(hydroxymethyl)aminomethane (Tris) buffer (0.5 M) at 25 °C for 4 h. The reaction was stopped by adding 1.0 mL of 25% barium acetate followed by 10 mL of 95% ethyl alcohol. An off-white precipitate was removed by centrifugation. Additional 95% ethanol (100 mL) was added before storing the solution at 4 °C for 3 h. The barium salt of NADH was collected by centrifugation and the pellet suspended in absolute ethanol. The supernatant was discarded after centrifugation. Similar rinses with a 1:1 mixture of absolute ethanol–diethyl ether and then diethyl ether gave a yellowish precipitate. Immediate drying in a vacuum desiccator over $CaCl_2$ produced 0.16 g of product (67% yield). The 250-MHz ^{1}H NMR in D_2O confirmed >95% deuteration at C-4 of NADH by comparison of the peak integrals at C-4 (σ = 6.9

Scheme I: Chemical Modification of Enzymatically Derived [2-^{3}H](Dihydroxyphenyl)ethyl Alcohols to [2-^{3}H]Dopamines

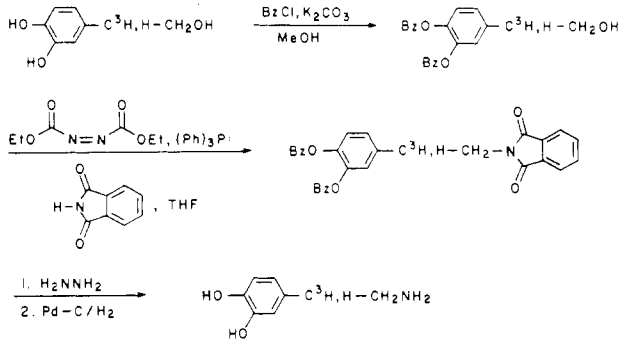

ppm) and C-2 (σ = 2.7 ppm) of the nicotinamide ring. The peak ratio, C-4 to C-2, was 1.93 for NADH and 0.99 for NADD.

Synthesis of [1-^{2}H]Cyclohexanol. Freshly distilled cyclohexanone, 2.1 mL (20 mmol), dissolved in 40 mL of 0.1 N NaOH was dripped slowly into a solution of 2.5 g of $NaBD_4$ in 10 mL of 0.1 NaOH. The reaction was stopped after 5.0 h by the addition of 3.0 N HCl. Crystalline sodium chloride was added and the aqueous solution extracted with ether (6 × 35 mL). The ether extracts were dried over anhydrous Na_2SO_4 and filtered before the solvent was removed under vacuum. The remaining crude product was distilled under vacuum (18 Torr) with the [1-^{2}H]cyclohexanol being collected in the fraction distilling at 62–63 °C. The 90-MHz ^{1}H NMR in $CDCl_3$ showed at least 95% deuteration at the C-1 position.

Enzymatic Preparation of [1(R)-^{2}H,2(R)-^{3}H]-2-(3,4-Dihydroxyphenyl)ethyl Alcohol. The barium salt of [4(*R*)-^{2}H] NADH was converted to the sodium salt by adding a slight excess of sodium sulfate to a 15 mM solution of cofactor. The barium sulfate that forms was removed by centrifugation.

A reaction mixture containing 10 μmol of dopamine, 1.4 μmol of [4(*R*)-^{2}H]NADH, 20 μmol of [1-^{2}H]cyclohexanol, 0.4 mg of catalase (39000 units/mg), 2.5 units of liver alcohol dehydrogenase (1.6 units/mg), and 0.20 unit of plasma amine oxidase (0.14 unit/mg) in a total volume of 0.85 mL containing tritiated water with a final specific activity = 8.7 × 10^6 cpm/μmol was incubated for 9 h at 25 °C. Following removal of tritiated water and deproteinization, [1(*R*)-^{2}H,2(*R*)-^{3}H]-2-(3,4-dihydroxyphenyl)ethyl alcohol was isolated by semipreparative reverse-phase HPLC. A total of 4.7 μmol of alcohol product with a specific activity = 6.9 × 10^6 cpm/μmol was collected and diltued with cold 2-(3,4-dihydroxyphenyl)ethyl alcohol to a final specific activity of 3.0 × 10^4 cpm/μmol. Solvent was removed in vacuo and the residue dried in a vacuum desiccator over P_2O_5.

Conversion of 2-(3,4-Dihydroxyphenyl)ethyl Alcohols to 2-(3,4-Dihydroxyphenyl)ethylamines. The general procedure for the chemical conversion of the above [2(*R*)-^{3}H]-2-(3,4-dihydroxyphenyl)ethyl alcohols to the corresponding [2(*R*)-^{3}H]-2-(3,4-dihydroxyphenyl)ethylamines is described below for the synthesis of dopamine protonated at C-1 (Scheme I).

Protection of 2-(3,4-Dihydroxyphenyl)ethyl Alcohol. The tritiated 2-(3,4-dihydroxyphenyl)ethyl alcohol was dried over P_2O_5 in a vacuum desiccator overnight. A total of 2.5 g of anhydrous K_2CO_3 followed by the dropwise addition of 2.3 mL of distilled benzyl chloride in 5.0 mL of absolute methanol was added to a methanol solution (5.0 mL) of the alcohol. After refluxing overnight under dry nitrogen gas, the solvent was removed in vacuo, leaving a residue that was partitioned between H_2O (20 mL) and ether (20 mL). The aqueous layer was extracted with additional ether (3 × 20 mL). The combined organic phases were washed with water and saturated brine and dried over anhydrous $MgSO_4$. Removal of the ether in vacuo gave a yellow oil, which was applied to a small silica column (1.0 × 24 cm) and eluted with benzene at a flow rate of 1.0 mL/min. A total of 0.3 g of tritiated 2-[3,4-bis(benzyloxy)phenyl]ethyl alcohol was recovered. ^{1}H NMR in $CDCl_3$ showed the following: δ 1.5 (s, br, H), 2.8 (t, 2 H), 3.8 (t, 2 H), 5.1 (s, split, 4 H), 6.8 (m, 3 H), and 7.4 (m, 10 H).

Conversion of 2-[3,4-Bis(benzyloxy)phenyl]ethyl Alcohol to [2-[3,4-Bis(benzyloxy)phenyl]ethyl]phthalimide. To the preceding protected [bis(benzyloxy)phenyl]ethyl alcohol in 2.0 mL of freshly distilled dry THF were added 0.15 g (1 mmol) of phthalimide and 0.26 g (1 mmol) of triphenylphosphine. A total of 0.16 mL (1 mmol) of diethyl azidocarboxylate in 1.0 mL of THF was dripped slowly into the stirring reaction mixture. After overnight reaction at room temperature, the THF was removed by rotary evaporation. A 2.0-mL solution of the residue in $CHCl_3$ was loaded on a silica gel column (2.5 × 21 cm), containing 36 g of adsorbent. Elution with $CHCl_3$ gave 0.25 g of phthalimide adduct (60% yield). The 90-MHz ^{1}H NMR in $CDCl_3$ showed the following: δ 2.9 (t, 2 H), 3.9 (t, 2 H), 5.1 (s, split, 4 H), 6.8 (m, 3 H), 7.4 (m, 10 H), and 7.8 (m, 4 H).

Hydrazinolysis of [2-[3,4-Bis(benzyloxy)phenyl]ethyl]-phthalimide. A total of 0.25 g (0.54 mmol) of the above phthalimide adduct was reacted with a 4-fold excess of hydrazine hydrate in ethanol. A slurry of the reactants in 2.0 mL of ethanol was stirred until the solution began clearing, indicating formation of the initial soluble phthalimide–hydrazine intermediate. Another 5.0 mL of ethanol was added to provide ample solvent for suspending the insoluble phthalhydrazide as it formed. The mixture was refluxed for 5 h followed by the addition of several drops of concentrated HCl. The residue obtained after solvent removal in vacuo was partitioned between H_2O and $CHCl_3$. A total of 0.050 g (0.15 mmol) of crude 2-[3,4-bis(benzyloxy)phenyl]ethylamine hydrochloride was recovered from drying the combined organic phases.

Deprotection of 2-[3,4-Bis(benzyloxy)phenyl]ethylamine. The crude [bis(benzyloxy)phenyl]ethylamine, without further purification, was dissolved in 5.0 mL of 95% ethanol containing 3 drops of 3.0 N HCl. A total of 40 mg of palladized charcoal (10%) was added and hydrogenolysis carried out with 1 atm of hydrogen gas at ambient temperature. When hydrogen uptake was complete, the catalyst was removed by filtration and rinsed with several small portions of methanol. Evaporation of the filtrate produced the slightly discolored tritiated dopamine. Further purification by semipreparative reverse-phase HPLC in a mixture of 95% acetic acid (1%)–5% methanol gave 180 mg of [2(*R*)-^{3}H]dopamine with a specific activity of 1.1 × 10^4 cpm/μmol, 10% overall yield from 2-(3,4-dihydroxyphenyl)ethyl alcohol.

Synthesis of [1(R)-^{2}H,2(R)-^{3}H]- and [1(S)-^{2}H,2(R)-^{3}H]-Dopamines. Chemical modification of the [1(*S*)-^{2}H,2(*R*)-^{3}H]- and [1(*R*)-^{2}H,2(*R*)-^{3}H]-2-(3,4-dihydroxphenyl)ethyl alcohols followed the same procedure described for the synthesis of [2(*R*)-^{3}H]dopamine. A total of 60 μmol of [1(*R*)-^{2}H,2-(*R*)-^{3}H]dopamine with specific activity = 1.4 × 10^4 cpm/μmol and 100 μmol of [1(*S*)-^{2}H,2(*R*)-^{3}H]dopamine with specific activity 2.8 × 10^4 cpm/μmol were isolated by semipreparative HPLC after all chemical transformations.

Analysis of Tritium Release from [2-^{3}H]Dopamines with Dopamine β-Hydroxylase. Tritiated dopamines were incubated in solutions containing 5 μmol of fumarate, 5 μmol of

Table I: Extent of Tritium Incorporation at C-2 of Product during Dopamine Oxidation by Plasma Amine Oxidase

reactants[a]			product alcohols[b]	
dopamine	NADH	TOH (cpm/μmol)	configuration	cpm/μmol
1-^{1}H	4-^{1}H	2.3×10^6	2-^{3}H	2.0×10^6
1(*S*)-^{2}H	4-^{1}H	3.7×10^6	1(*S*)-^{2}H,2-^{3}H	3.6×10^6
1-^{1}H	4(*R*)-^{2}H	8.7×10^6	1(*R*)-^{2}H,2-^{3}H	6.9×10^6

[a] The preparation of [1(*S*)-^{2}H]dopamine and [4(*R*)-^{2}H]NADH and the conversion of dopamines to 2-(3,4-dihydroxyphenyl)ethyl alcohols are described under Methods. [b] 2-(3,4-Dihydroxyphenyl)ethyl alcohol.

ascorbate, 80 μg of catalase, 1.25 nmol of $CuCl_2$, 0.85 nmol of dopamine β-hydroxylase (containing 0.4 Cu/subunit), and 50 μmol of sodium acetate buffer, pH 5.5, in a total volume of 0.5 mL. After 3 h, 0.1 mL of the reaction mixture was added to an equal volume of 5% $HClO_4$ and assayed for norepinephrine production by fluorescence analysis as described by Krueger and Klinman (1982). Tritiated water was separated from labeled product by bulb-to-bulb distillation in vacuo of frozen acidified reaction mixtures. Residue and volatile portions were counted in 30% ethanol/toluene or 30% surfactant/toluene cocktails.

Analysis of Tritium Release from [2-^{3}H]Dopamines with Plasma Amine Oxidase. The extent of tritium release to solvent during substrate oxidation was examined in incubations of C-2-tritiated dopamines with plasma amine oxidase. Reaction mixtures contained 0.8 mg of catalase (39 000 units/mg), 3.0 units of liver alcohol dehydrogenase (1.6 unit/mg), 0.20 unit of plasma amine oxidase (0.15 unit/mg), 4 μmol of cyclohexanol, 2.2 μmol of NADH, 2 μmol of [2-^{3}H]dopamine, and 200 μmol of sodium phosphate, pH 7.0, in a total volume of 2.0 mL. Aliquots were removed at various times, deproteinized by ultrafiltration, and assayed for product formation by HPLC. Analysis involved replicate 20-μL injections onto an analytical reverse-phase column (4.6 mm × 25.0 cm), equilibrated with a mobile phase of 95% acetic acid (1%)–5% methanol at 1.0 mL/min. Elution was monitored at 280 nm, and product levels were determined by comparing peak area integrations with those of standard solutions. Percentage volatile tritium was determined by separating volatile and residue portions of frozen reaction aliquots by bulb-to-bulb distillation. The ratios of percent tritium release to product formation were corrected for values obtained in simultaneous control reactions.

Results

Tritium Incorporation at C-2 of Dopamines. Incubation of plasma amine oxidase with [2-^{3}H]dopamine has previously been shown to lead to a nonstereospecific and rapid loss of tritium to solvent (Summers et al., 1979). In the present experiments, substrate was oxidized by enzyme in the presence of tritiated water. As shown in eq 3, aldehyde was reduced

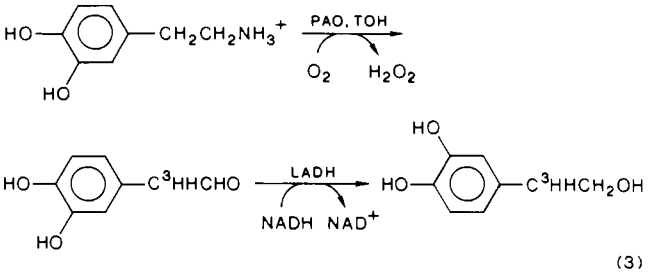

(3)

to alcohol, in a coupled NADH/alcohol dehydrogenase system, to prevent any nonenzymatic exchange at the β-position of product. In eq 3, PAO and LADH are plasma amine oxidase and horse liver alcohol dehydrogenase, respectively. In Table I, the specific activities of [2-^{3}H]-2-(3,4-dihydroxyphenyl)ethyl alcohols so obtained are compared to the specific activities of tritiated water used in reaction mixtures. As seen, there is close agreement in specific activities, indicating essentially complete exchange of tritium from solvent into product.

Table II: Specific Activity of Dopamines and Their Alcohol Precursors (Scheme I)

precursor alcohols[a]		product amines	
configuration	cpm/μmol[b]	configuration	cpm/μmol
2-^{3}H	1.2×10^3	2-^{3}H	1.1×10^3
1(*S*)-^{2}H,2-^{3}H	1.3×10^4	1(*R*)-^{2}H,2-^{3}H	1.3×10^4
1(*R*)-^{2}H,2-^{3}H	3.0×10^4	1(*S*)-^{2}H,2-^{3}H	2.8×10^4

[a] 2-(3,4-Dihydroxyphenyl)ethyl alcohols were converted to dopamines as described under Methods. [b] Determined after diluting purified, enzyme-generated [2-^{3}H]-2-(3,4-dihydroxyphenyl)ethyl alcohols with cold carrier to produce 1 mmol.

Table III: Stereochemical Analysis of Tritium at C-2 of [2-^{3}H]Dopamine[a]

dopamine	volatile (cpm)	residue (cpm)	% volatile (*pro-R*)[b]
2-^{3}H	502	26	95
1(*R*)-^{2}H,2-^{3}H	2070	115	95
1(*S*)-^{2}H,2-^{3}H	2530	324	88

[a] Dopamine was incubated with dopamine β-hydroxylase, as indicated under Methods. [b] Values of percent volatile were corrected for background counts measured in simultaneous control reactions. All values are those measured at 100% reaction.

In the original experiments of Summers et al. (1979), an unexpected lack of stereospecificity was observed in both the oxidation (at C-1) and exchange (at C-2) reactions of dopamine. In an effort to determine the stereochemical path for tritium incorporation, [2-^{3}H]-2-(3,4-dihydroxyphenyl)ethyl alcohols were converted to [2-^{3}H]dopamine by the chemical sequence outlined under Methods (Scheme I), followed by incubation with dopamine β-hydroxylase (*pro-R* specific at C-2 of dopamine). In the chemical conversion of Scheme I, tritiated alcohols were diluted with cold carrier to yield the specific activities of Table II. As shown, the specific activities of the final dopamine products are in close agreement with the alcohol precursors. This is an important control, indicating little or no tritium loss in the conversion of alcohol to amine. As an additional control for exchange and/or racemization at the β-position of substrate in the alcohol to amine conversion, [2,2-^{2}H$_2$]-2-[3,4-bis(benzyloxy)phenyl]ethyl alcohol was converted to amine by Scheme I. Analysis of product by NMR indicated no change in signal intensity for the α-protons (ruling out carbon interchange on the ethyl side chain) and no detectable signal arising from the β-position (ruling out exchange).

Stereochemical analysis of tritium incorporated into the C-2 position of dopamine was carried out with dopamine β-hydroxylase and yielded the results in Table III. As seen, exchange occurs in a *stereospecific manner*, leading almost exclusively to 2(*R*)-^{3}H products for dopamine oxidation by plasma amine oxidase. We note a slight reduction in stereospecificity when dopamine oxidation by plasma amine oxidase was coupled to [4(*R*)-^{2}H]NADH and liver alcohol dehydrogenase, leading to the [1(*S*)-^{2}H]dopamine product. Since this reaction was otherwise identical with the original dopamine experiment (first row, Table III), the decrease in stereospecificity is most likely due to insufficient trapping of intermediate aldehyde by deuterated coenzyme, i.e., some spontaneous

Chart I: Alternative Binding Modes for Oxidation of Dopamine by Plasma Amine Oxidase[a]

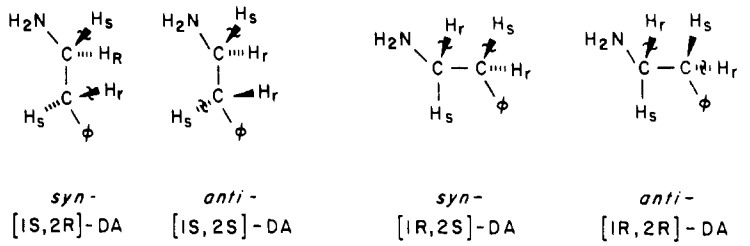

[a] Within each mode, the hydrogen abstracted from C-1 can be cleaved either syn (same side of ethyl side chain) or anti (opposite side) with respect to the hydrogen removed at C-2, thereby creating four possible structures.

Table IV: Incubation of [2(*R*)-^{3}H]Dopamines with Plasma Amine Oxidase[a]

dopamine	% P[b]	tritium (cpm) volatile	residue	% V[c]	% V/P
2(*R*)-^{3}H	29	67	412	14	46
	91	174	236	42	46
1(*S*)-^{2}H,2(*R*)-^{3}H	53	146	1090	12	20
	100	821	3510	19	18
1(*R*)-^{2}H,2(*R*)-^{3}H	28	124	758	14	42
	56	226	586	28	46
	94	448	353	56	57
	100	628	264	70	68

[a] Dopamines were incubated with plasma amine oxidase as described under Methods. [b] Percent product formation. [c] Percent volatile counts.

exchange of 3,4-dihydroxyphenacetaldehyde prior to its reduction to alcohol.

Tritium Release from [2(R)-^{3}H]Dopamines. The observation of a close to absolute stereospecificity for the washin of tritium into the β-position of dopamine, Table III, contrasts sharply with the random loss of label from [2-^{3}H]dopamine reported by Summers et al. (1979). Thus, [2(*R*)-^{3}H]dopamine samples were reincubated with plasma amine oxidase. As shown in Table IV, incubation of [2(*R*)-^{3}H]dopamine leads to a release of 47% of the tritium counts at C-2, analogous to the value of 42 ± 6% previously observed for the oxidation of [2(*R*)-^{3}H]dopamine. This result confirms the random release of tritium from chirally tritiated dopamine substrates reported by Summers et al. (1979) and indicates that tritium washin and release are not simply the microscopic reverse of one another.

Significantly, isotopic labeling at C-1 of dopamine introduces stereochemical selectivity in the release of tritium from the β-position of dopamine during oxidation. As seen in Table IV, deuteration in the *pro-S* position at C-1 of dopamine reduces the amount of volatile tritium ca. 2-fold, whereas deuteration in the *pro-R* position leads to a significant enhancement in tritium release. It should be noted that the ratio of tritium release to product formation is time-independent for [2(*R*)-^{3}H]- and [1(*S*)-^{2}H,2(*R*)-^{3}H]dopamine, whereas the percent V/P rose from 42% to 68% with the 1(*R*)-^{2}H,2(*R*)-^{3}H sample. As considered under Discussion, this time dependence can be rationalized by the generation of ca. 10% undeuterated substrate in the course of [1(*R*)-^{2}H,2(*R*)-^{3}H]dopamine synthesis.

Discussion

Stereochemical Relationship between Bond Cleavage at C-1 vs. C-2 of Dopamine. In the original model of Summers et al. (1979), dopamine was proposed to be processed via alternate binding modes having absolute but opposing stereochemistries, shown in Chart I for cleavage of the *pro-S* vs. *pro-R* hydrogens at C-1 with either a syn or anti relationship between the bond cleavages at C-1 and C-2. Additional features of importance to the present study were, first, the finding of approximately equal flux rates for dopamine oxidation via modes *S* and *R* and, second, the demonstration of a large differential in primary isotope effects at C-1 with [1(*S*)-^{3}H]dopamine yielding $^T(V/K)$ = 26–34 and [1(*R*)-^{3}H]dopamine yielding $^T(V/K)$ = 4.4–6.4. In this study, we have used these differences in kinetic isotope effects to *alter* flux rates for substrates in a predictable way. Thus, deuteration in the *pro-S* position at C-1 is expected to lead to oxidation primarily by *pro-R* cleavage (*R*:*S* ≃ 0.9:0.1), while deuteration in the *pro-R* position can be used to give preferential *pro-S* cleavage (*S*:*R* ≃ 0.75:0.25).

Table V: Predicted Percent Tritium Release from [2(*R*)-^{3}H]Dopamine, as a Function of Deuteration at C-1[a]

dopamine	C-1/C-2 relationship syn (%)	anti (%)
1(*R*)-^{2}H,2(*R*)-^{3}H	74	21
1(*S*)-^{2}H,2(*R*)-^{3}H	8	90

[a] Calculated from previous studies of (i) primary tritium isotope effects for the plasma amine oxidase oxidation of [1(*R*)-^{3}H]- and [1-(*S*)-^{3}H]dopamine and (ii) the extent of exchange from [2(*R*)-^{3}H]- and [2(*S*)-^{3}H]dopamines [cf. Summers et al. (1979) and the Appendix].

Inspection of Chart I indicates that under the circumstance of preferential fluxes the stereochemistry of tritium release from C-2 of dopamine will indicate the stereochemical relationship between C-1 and C-2; for example, oxidation of [1-(*S*)-^{2}H]dopamine largely by the 1*R* mode is expected to release tritium from the 2*S* position for a syn relationship and from the 2*R* position for an anti relationship.[1] This point is elaborated further in Table V, where the expected release of tritium from [2(*R*)-^{3}H]dopamines is shown to be coupled to isotopic labeling. As seen, the expected percent of tritium release for [1(*R*)-^{2}H]- and [1(*S*)-^{2}H]dopamine is reversed

[1] The relationship between C–H bond cleavage at C-1 and C-2 pertains to the conformations drawn in Chart I. These conformations were previously described by Summers et al. (1979) and had been constructed in order to (i) maintain close to identical binding sites for the amine nitrogen and C–H bond undergoing cleavage in both benzylamine and the two conformers of dopamine, (ii) allow for similar interactions between the catechol ring and enzyme for both conformers of dopamine, and (iii) place the H_S and H_R hydrogens at C-1 and hydrogens at C-2 of the dopamine conformers as close together as possible. Alternate conformations are highly unlikely but are conceivable, for example, conformations involving a 180° rotation about the C-1–C-2 bond of dopamine. We note that this particular type of rotation would lead to a wide disparity between the catechol binding sites as the hydrogens at C-2 of the two conformers approach one another. Additionally, such a bond rotation generates considerable crowding between the catechol ring of the 1*R* conformer and the pyridine ring of the putative cofactor.

from 21% and 90% for an anti cleavage to 74% and 8%, respectively, for a syn process. The analysis in Table V, which requires chiral tritiation of dopamine at C-2, is based on 2-(*R*)-^{3}H samples, since as shown in Table III plasma amine oxidase catalyzes a stereospecific incorporation into the *pro-R* position at C-2, providing a relatively straightforward synthetic route for the preparation of [1(*S*)-^{2}H,2(*R*)-^{3}H]- and [1-(*R*)-^{2}H,2(*R*)-^{3}H]dopamine samples.

With the observed percentage of tritium release of 68% for [1(*R*)-^{2}H,2(*R*)-^{3}H]dopamine and 18% for [1(*S*)-^{2}H,2(*R*)-^{3}H]dopamine (Table V), the data indicate that a syn relationship exists for C–H bond cleavage. However, some discrepancy exists between expected and observed values of tritium release from multilabeled substrates, and this must be explained. First, oxidation of [1(*R*)-^{2}H,2(*R*)-^{3}H]dopamine proceeded with a time-dependent release up to 68% of the tritium at C-2, compared to the expected value of 74%. We attribute this to incomplete deuteration of substrate at C-1, since the sample of [1(*R*)-^{2}H,2(*R*)-^{3}H]dopamine was derived from the reaction of [1(*S*)-^{2}H]dopamine with plasma amine oxidase. Given the syn relationship between proton activation at C-1 and C-2, an isotope effect of 9.6 exists for cleavage of the *pro-S* position at C-1 (Summers et al., 1979). Thus, catalysis is expected to occur with approximate flux ratios of 0.9 for 1*R* cleavage and 0.1 for 1*S* cleavage, and roughly 10% of deuterium at C-1 will be released to solvent as the substrate undergoes oxidation. Overall, the final pool of [1(*R*)-^{2}H,2-(*R*)-^{3}H]dopamine should contain 90% [1(*R*)-^{2}H,2(*R*)-^{3}H]-dopamine molecules with the remaining 10% being [2(*R*)-^{3}H]dopamine. Incubation of this mixture of [2-^{3}H]dopamines with plasma amine oxidase creates a competition between these two substrates for the enzyme. Since there is no isotope effect on oxidation of [2(*R*)-^{3}H]dopamine, it will undergo catalysis at a faster rate than [1(*R*)-^{2}H,2(*R*)-^{3}H]dopamine, such that tritium release at early times will follow the kinetics of [2-(*R*)-^{3}H]dopamine exchange (random) while at longer reaction times the ratio of tritium release to product formation will reflect the oxidation of [1(*R*)-^{2}H,2(*R*)-^{3}H]dopamine (74:26). Thus, an external competition between [2(*R*)-^{3}H]dopamine and [1(*R*)-^{2}H,2(*R*)-^{3}H]dopamine leads to the observed time-dependent ratio of tritium release to product formation observed during substrate oxidation (Table IV). At 100% conversion, the final ratio is somewhat reduced relative to the value calculated for fully deuterated [1(*R*)-^{2}H,2(*R*)-^{3}H]dopamine, since a slight excess of tritium is carried into product during the nonstereospecific oxidation of [2(*R*)-^{3}H]dopamine.

As seen from Tables IV and V, the observed 18% tritium release from [1(*S*)-^{2}H,2(*R*)-^{3}H]dopamine is an overestimate. All molecules in this substrate pool are fully deuterated at C-1 since deuterium incorporation was achieved by enzymatic reduction of the aldehyde with [4(*R*)-^{2}H]NADH. Tritium exchange at C-2, however, was not absolutely stereospecific. Incubation of [1(*S*)-^{2}H,2(*R*)-^{3}H]dopamine with dopamine β-hydroxylase revealed only 88% *pro-R* incorporation of label at C-2. Presumably, the other 12% of the tritium has the *pro-S* configuration at C-2, reflecting spontaneous exchange of the aldehyde with solvent before its reduction to the alcohol [cf. Lovenberg and Beaven (1971)]. If this is assumed to be correct, the sample of dopamine actually consists of 88% [1-(*S*)-^{2}H,2(*R*)-^{3}H]dopamine and 12% [1(*S*)-^{2}H,2(*S*)-^{3}H]dopamine. The relative flux for [1(*S*)-^{2}H]dopamine through the 1*S* mode is 10% with the majority of catalysis, 90%, occurring with 1*R* hydrogen removal at C-1 and *pro-S* abstraction at C-2. We calculate the percentage of tritium released from the pool of [1(*S*)-^{2}H,2-^{3}H]dopamines as the sum of (0.90)(0.12) = 0.11 for oxidation of [1(*R*)-^{1}H,2(*S*)-^{3}H]dopamine and (0.10)(0.88) = 0.088 for oxidation of [1(*S*)-^{2}H,2-(*R*)-^{3}H]dopamine for a total of 19.6%. Our measured percentage of tritium release of 18% coincides nicely with this projection. Thus, the data strongly support the conclusion that the relationship between C-H bond cleavage at C-1 and C-2 is syn.

Chart II: Structure of Schiff Base Formed between Proposed Cofactor Pyrroloquinoline Quinone and Benzylamine

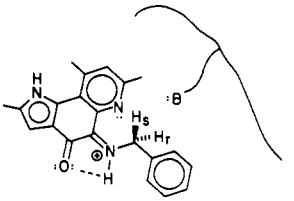

Stereochemical Relationship between Tritium Incorporation and Exchange from C-2 of Dopamine. Whereas unlabeled [2(*R*)-^{3}H]dopamine shows nonstereospecific release of tritium from C-2, specificity is introduced into the exchange reaction by deuteration at C-1. This observation corroborates earlier studies, which proposed mirror-image catalysis for dopamine, as shown in Chart I. In fact, the initial isotope effects reported by Summers et al. (1979) proved to be accurate enough to allow the prediction of tritium release ratios for the oxidation of [1(*R*)-^{2}H,2(*R*)-^{3}H]dopamine and [1(*S*)-^{2}H,2(*R*)-^{3}H]dopamine.

A dilemma arises however when tritium incorporation and exchange are compared. As seen in Table III, specific tritium incorporation occurs for all dopamine substrates studied, whereas random tritium release from C-2 occurred during the oxidation of [2-^{3}H]dopamines [Table IV and Summers et al. (1979)]. These observations appear to violate the principle of microscopic reversibility, which necessitates equivalent mechanisms for the forward and reverse directions of a reaction. Thus, we must conclude that enamine protonation is not simply the microscopic reverse of imine exchange.

In an effort to understand this apparent conflict, we have constructed models of the plasma amine oxidase active site using the recently proposed cofactor pyrroloquinoline quinone as a frame of reference. Starting with the *pro-S*-specific substrate (benzylamine) and allowing for covalent adduct formation and hydrogen binding of the substrate-derived imine to the carbonyl of cofactor, we obtain the structure shown in Chart II. An unexpected feature of this structure is that *pro-S* hydrogen abstraction can only be effected by a basic residue lying *above the plane* defined by substrate and cofactor. Rotation about the C–N bond, such that the *pro-S* hydrogen points below this plane, leads to a collision of the benzene ring of substrate and pyridine ring of cofactor. From previous studies of base catalysis in the plasma amine oxidase reaction, we have proposed a transfer of hydrogen from substrate to cofactor in the course of substrate oxidation (Farnum et al., 1985):

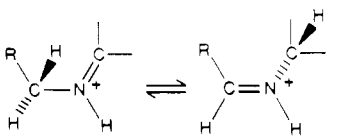

(4)

Thus, as long as hydrogen bonding occurs as indicated in Chart II, we predict that cofactor will undergo protonation at the *re* face of C-5. Alternatively, in the event that the substrate imine hydrogen bonds to the pyridine nitrogen of cofactor, the *si* face of cofactor would be attacked. It will be of considerable

Chart III: Structures for 1(*S*),2(*R*)-Dopamine Complexed to Pyrroloquinoline Quinone[a]

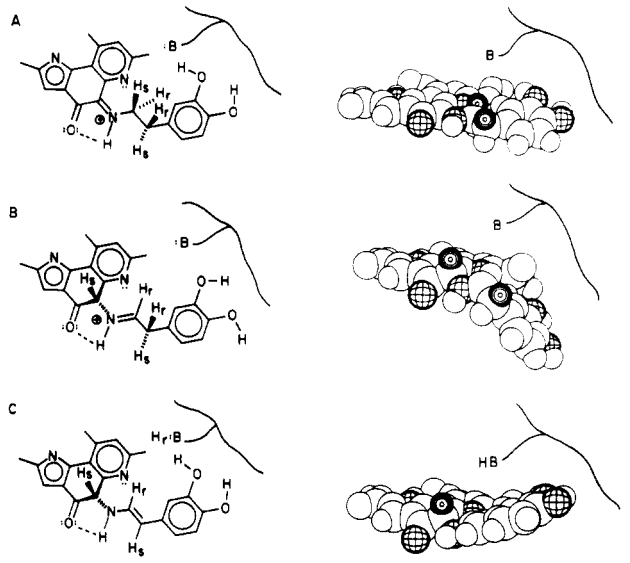

[a] (A) The covalent enzyme substrate complex E_{ox}·S; (B) imine formed upon enzyme reduction, E_{red}·imine; (C) enamine resulting from proton abstraction in (B), E_{red}·enamine. Each of the intermediates is shown with stick models (left) and computer-generated space-filling models (right).

interest to see if hydrogen transfer to cofactor can be detected and characterized stereochemically, allowing an unambiguous determination of substrate orientation in the active site.

The structures of dopamine, complexed to pyrroloquinoline quinone, have also been constructed in Charts III and IV. Beginning with the 1*S*,2*R* binding mode of dopamine in Chart III, we trace the conversion of the initial E_{ox}·S complex (A) to reduced enzyme E_{red}·imine (B) to E_{red}·enamine (C). As shown, these transformations are catalyzed by a single residue (Farnum et al., 1985) in a syn fashion (this study). Importantly, each interconversion can occur facilely, without the introduction of steric strain between cofactor and substrate and with the substrate lying either in or below the plane defined by pyrroloquinoline quinone. Of additional note is the formation of a trans configuration about the imine bond in E_{red}·imine.

The interaction of the 1*R*,2*S* binding mode of dopamine is contrasted with 1*S*,2*R* in Chart IV. In constructing this alternate mode, we observe increasing movement of the phenyl ring of substrate from below to above the pyrroloquinoline quinone plane. Initially, introduction of substrate into E_{ox}·S (A) can be accomplished without significant strain by allowing substrate to be bound below the cofactor plane. In this mode, abstraction of the *pro-R* hydrogen at C-1 leads to E_{red}·imine (B) with a cis geometry about the new imine bond. It is important to note that we are unable to bind the 1(*R*),2(*S*)-dopamine in such a way as to obtain a trans geometry following substrate oxidation. A feature that follows from the cis geometry is that substrate is forced to lie significantly above the pyrroloquinoline quinone plane. In fact, the displacement becomes even more severe when E_{red}·imine (B) is converted to E_{red}·enamine (C). While the cis geometry in Chart IVB is almost certainly more hindered than the trans geometry in Chart IIIB, isomerization about the imine double bond is prohibited. Proton abstraction from the β-carbon to form E_{red}·enamine (Chart IVC), however, generates a species that can freely rotate about the C–N bond, to generate the structure obtained upon 1*S*,2*R* oxidation (Chart IIIC). It would appear that the observation of a stereospecific incorporation of label

Chart IV: Structures for 1(*R*),2(*S*)-Dopamine Complexed to Pyrroloquinoline Quinone[a]

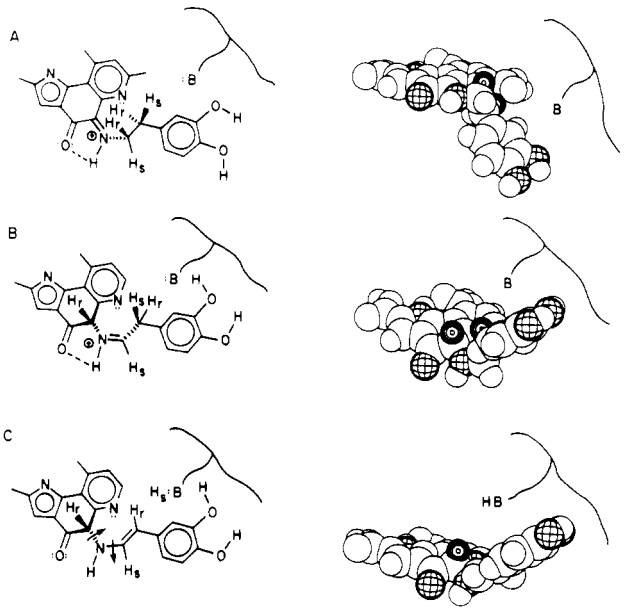

[a] (A) Covalent enzyme substrate complex, E_{ox}·S; (B) imine formed upon enzyme reduction, E_{red}·imine; (C) enamine resulting from proton abstraction in (B), E_{red}·enamine. Each of the intermediates is shown with stick models (left) and computer-generated space-filling models (right).

from solvent is a simple consequence of enamine destabilization in the oxidation of 1(*R*),2(*S*)-dopamine. Rapid conversion of this enamine to the 1*S*,2*R* form results in a common intermediate, which upon protonation generates the 2(*R*)-^{3}H product.[2]

It is of some interest that the more hindered substrate 1-(*R*),2(*S*)-dopamine exhibits a smaller steady-state isotope effect on V_{max}/K_m than 1(*S*),2(*R*)-dopamine, $^D(V/K)$ = 3.6 and 9.6, respectively (Summers et al., 1979). Since imine conversion to enamine lies off the reaction path and substrate binding and release are fast, a reduction in $^D(V/K)$ from the intrinsic value, $^Dk_3 \simeq 12.5$, must arise either from a partially rate-limiting step following cofactor reduction or possibly from different intrinsic isotope effects. We consider the latter possibility unlikely since, first, $^Dk_3$ is observed to be essentially constant for a range of substrates (Palcic & Klinman, 1983) and, second, 1(*S*),2(*R*)- and 1(*R*),2(*S*)-dopamine are characterized by similar flux rates (Summers et al., 1979). Thus, we propose a partially rate-limiting conformational change prior to both proton exchange and imine hydrolysis, in the processing of the imine derived from 1(*R*),2(*S*)-dopamine (Chart IVB). We place this isomerization before the imine to enamine conversion, since the data in Tables IV and V indicate that tritium exchange from [1(*R*)-^{2}H,2(*R*)-^{3}H]dopamine follows the pattern expected for an isotope effect of 3.6

[2] Precedence for such a gain in stereospecificity in the course of substrate processing can be found in the literature, for example, the methylaspartase-catalyzed conversion of both *threo*- and *erythro*-methyl aspartate to mesoconate. To explain this result, Bright and Ingraham have invoked the formation of carbanionic intermediates of differential stability such that bond rotation in the intermediate derived from the erythro substrate, **1**, leads to the common threo intermediate, **2**, which upon C–N bond cleavage generates mesoconate:

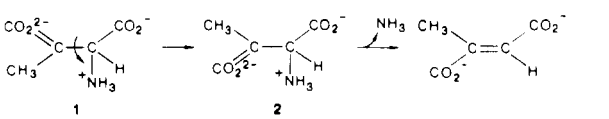

1 **2**

not 9.6. In the case of the 1*S*,2*R* substrate, the magnitude of $^{D}(V/K)$ is virtually at the intrinsic value, indicating that the *trans*-imine formed within this binding mode (Chart IIIB) is already correctly positioned for both a rapid hydrolysis and an even faster proton exchange rate.

Mirror-Image Catalysis. Although reports of a lack of stereospecificity in enzyme reactions exist in the literature, for example, the pyridoxamine-5′-phosphate oxidase catalyzed oxidation of pyridoxamine 5′-phosphate (Bowers-Komro & McCormick, 1985), these instances may represent a simple lack of discrimination between chiral centers, as opposed to the processing of substrate via alternate but stereospecific binding modes. The concept of mirror-image binding in enzyme catalysis stems from studies on diol dehydratase, in which Arigoni and co-workers demonstrated that either the *pro-R* or *pro-S* hydrogen at C-1 of propanediol was cleaved, depending on whether the substrate had the *R* or *S* configuration at C-2, **1** and **2**, respectively. This result has been attributed

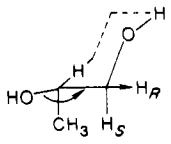

1

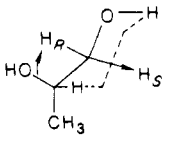

2

to the requirement for an anti-periplanar configuration between the migrating hydroxyl group and departing hydrogen. As shown, the relative positions of three possible binding sites, the primary and secondary hydroxyl groups and the methyl group, remain virtually unchanged in the two binding orientations. Further, both substrates are bound such that the cofactor can abstract and return the migrating hydrogen from the same side of the substrate. It appears that diol dehydratase represents a relatively novel example in which *substrate mirror images* are processed via mirror-image binding modes.

More recent studies by Kozarich and co-workers on glyoxylase have involved glutathione derivatives of glyoxylate, which force the reactive thiol hemiacetal to be bound in an inverted mode, **4**, relative to the natural substrate **3**, where

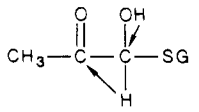

3

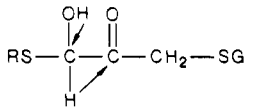

4

–SG represents glutathione and –SR represents a nonspecific, small thiol. For example, Kozarich and Chari (1982) have reported production of the L isomer of the thio ester from (glutathiomethyl)glyoxal and β-mercaptoethanol (**4**), whereas the D form of product arises when glutathione is used as the thiol reagent with glyoxylate (**3**). Although these results are attributed to mirror-image catalysis, they have, in fact, been artificially produced by binding the keto–aldehyde substrate in the "wrong" binding site. When glutathione is reacted with (glutathiomethyl)glyoxal, mostly D product is formed, suggesting that normal binding is favored (Kozarich et al., 1982).

Turning to this study, convincing evidence for the existence of two catalytic binding modes for dopamine at the active site of plasma amine oxidase has been presented (Tables IV and V). As illustrated in Charts III and IV, each mode is characterized by absolute but opposite stereochemistry for proton activation at C-1 and C-2. Further, a syn stereochemical relationship exists between the reactions at C-1 and C-2, which together with pK_a assignments (Farnum et al., 1986), implicates a single base in the catalysis of proton transfer between substrate and cofactor and in the exchange of the C-2 hydrogen with solvent. In this respect, plasma amine oxidase appears similar to diol dehydratase, since both enzymes are characterized by proton migrations between reaction centers from the same side of substrate, independent of the absolute chirality of the bonds undergoing cleavage. A clear-cut distinction between plasma amine oxidase and diol dehydratase does arise, however, in that the plasma amine oxidase processes the *identical substrate* by mirror-image binding modes. This observation appears to be a rare one in enzymology and is even more remarkable in that dopamine proceeds through the alternate modes with approximately equal flux rates (Summers et al., 1979).

Table VI: Predicted Loss of Tritium from [1(*S*)-^{2}H,2(*R*)-^{3}H]- and [1(*R*)-^{2}H,2(*S*)-^{3}H]Dopamines

	relationship between C-1 and C-2[a]			
	syn		anti	
	1*R*,2*S* mode	1*S*,2*R* mode	1*R*,2*R* mode	1*S*,2*S* mode
flux for [1(*S*)-^{2}H]dopamine	0.925	0.075	0.90	0.10
expected ^{3}H release from [1(*S*)-^{2}H,2(*R*)-^{3}H]dopamine (%)		7.5	90	
flux for [1(*R*)-^{2}H]dopamine	0.26	0.74	0.21	0.79
expected ^{3}H release from [1(*R*)-^{2}H,2(*R*)-^{3}H]dopamine (%)		74	21	

[a] A pictorial representation of these modes is given in Chart I in the text.

ACKNOWLEDGMENTS

We give special thanks to Professor Richard Mathies, Department of Chemistry, University of California at Berkeley, for the use of his computer facilities in generating the graphic displays.

APPENDIX

Derivation of Flux Rates for Dopamine Substrates. Enzymatic oxidation of dopamine by bovine plasma amine oxidase represents a partitioning of substrate between two competing reactions, *pro-R* or *pro-S* hydrogen abstraction at C-1. As shown, k_1 and k_2 are net rate constants defining the rate of catalysis through the 1*R* and 1*S* modes, respectively:

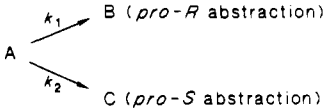

It follows that the ratio of product aldehydes, B to C, at 100% conversion, is equal to the ratio of net rate constants:

$$B_\infty/C_\infty = k_1/k_2$$

As described by Summers et al. (1979), the percentage of tritium released to solvent during oxidation of chirally labeled [2-^{3}H]dopamines is a measure of the relative flux of substrate through the two modes. The relative magnitudes of the flux rates depend to a small extent upon the stereochemical relationship between proton activation at C-1 and C-2, where the ratio of flux rates for 1*R* vs. 1*S* is 0.56:0.44 for syn cleavage or 0.44:0.56 for anti cleavage.

Substrates deuterated at C-1 should deviate significantly from the ca. 50:50 flux pattern, turning over predominantly

in the binding mode in which hydrogen is removed rather than deuterium. For example, [1(*S*)-^{2}H]dopamine will undergo catalysis at the same rate through the 1*R* mode but at a reduced rate through the 1*S* mode (proportional to an isotope effect of 9.6 or 11.6, depending upon the relationship between C-1 and C-2; Summers et al., 1979). As shown below, the relative flux rate of [1(*S*)-^{2}H]dopamine through the 1*R* vs. 1*S* mode is ca. 90:10. A similar calculation for [1(*R*)-^{2}H]-dopamine leads to relative flux rates of ca. 0.25:0.75.

Calculation of Flux Rates of [1(S)-^{2}H]Dopamine.

	syn cleavage	anti cleavage
1*R* mode	$k_1 = k_1$	$k_1 = k_1$
1*S* mode	$k_{2'} = k_2/9.6$	$k_{2'} = k_2/11.6$
$\frac{1R}{1R + 1S}$	$\frac{k_1}{k_1 + k_{2'}} = 0.925$	$\frac{k_1}{k_1 + k_{2'}} = 0.90$
$\frac{1S}{1R + 1S}$	$\frac{k_{2'}}{k_1 + k_{2'}} = 0.075$	$\frac{k_{2'}}{k_1 + k_{2'}} = 0.10$

Calculation of Flux Rates of [1(R)-^{2}H]Dopamine.

	syn cleavage	anti cleavage
1*R* mode	$k_{1'} = k_1/3.6$	$k_{1'} = k_1/3.0$
1*S* mode	$k_2 = k_2$	$k_2 = k_2$
$\frac{1R}{1R + 1S}$	$\frac{k_{1'}}{k_{1'} + k_2} = 0.26$	$\frac{k_{1'}}{k_{1'} + k_2} = 0.21$
$\frac{1S}{1R + 1S}$	$\frac{k_2}{k_{1'} + k_2} = 0.74$	$\frac{k_2}{k_{1'} + k_2} = 0.79$

As indicated in Table VI, tritium release from [1(*S*)-^{2}H,2-(*R*)-^{3}H]- and [1(*R*)-^{2}H,2(*R*)-^{3}H]dopamine is readily predicted from the flux rates given above.

References

Ameyama, M., Hayashi, M., Matsushita, K., Shinagawa, E., & Adachi, O. (1984) *Agric. Biol. Chem. 48*, 561–565.

Battersby, A. R., Staunton, J., & Summers, M. C. (1976) *J. Chem. Soc., Perkin Trans. 1*, 1052–1056.

Battersby, A. R., Staunton, J., Klinman, J. P., & Summers, M. C. (1979) *FEBS Lett. 91*, 297–298.

Bergin, R., & Carlstrom, D. (1968) *Acta Crystallogr., Sect. B: Struct. Crystallogr. Cryst. Chem. B24*, 1506–1510.

Bowers-Komro, D. M., & McCormick, D. B. (1985) *J. Biol. Chem. 260*, 9580–9582.

Bright, H. J., Lundin, R. E., & Ingraham, L. L. (1964) *Biochemistry 3*, 1224–1230.

Cruse, W. B. T., Kennard, O., & Salisbury, S. A. (1980) *Acta Crystallogr., Sect. B: Struct. Crystallogr. Cryst. Chem. B36*, 751–754.

Farnum, M. F., Palcic, M., & Klinman, J. P. (1986) *Biochemistry 25*, 1898–1904.

Henry, D. (1983) *Comput. Chem. 7*(3), 119–135.

Kozarich, J. W., & Chari, R. V. J. (1982) *J. Am. Chem. Soc. 104*, 2655–2657.

Lobensteen-Verbeek, C. L., Jongejan, J. A., Frank, J., & Divine, J. A. (1984) *FEBS Lett. 170*, 305–309.

Lovenberg, N., & Beaven, M. A. (1971) *Biochim. Biophys. Acta 251*, 452–455.

Mitsunobu, O. (1981) *Synthesis*, 1–28.

Palcic, M. M., & Klinman, J. P. (1983) *Biochemistry 22*, 5957–5966.

Retey, J., Umani-Ronchi, A., & Arigoni, D. (1966) *Experientia 22*, 72–73.

Rius, F. X., Knowles, P. F., & Pettersson, G. (1984) *Biochem. J. 220*, 767–772.

Summers, M. C., Markovic, R., & Klinman, J. P. (1979) *Biochemistry 18*, 1969–1979.

Suva, R. H., & Abeles, R. M. (1978) *Biochemistry 17*, 3538–3545.

Pyruvate Dehydrogenase and 3-Fluoropyruvate: Chemical Competence of 2-Acetylthiamin Pyrophosphate as an Acetyl Group Donor to Dihydrolipoamide†

Douglas S. Flournoy and Perry A. Frey*

Institute for Enzyme Research, The Graduate School, and Department of Biochemistry, College of Agricultural and Life Sciences, University of Wisconsin, Madison, Wisconsin 53705

Received December 30, 1985; Revised Manuscript Received June 3, 1986

ABSTRACT: The pyruvate dehydrogenase component (E_1) of the pyruvate dehydrogenase complex catalyzes the decomposition of 3-fluoropyruvate to CO_2, fluoride anion, and acetate. Acetylthiamin pyrophosphate (acetyl-TPP) is an intermediate in this reaction. Incubation of the pyruvate dehydrogenase complex with 3-fluoro[1,2-^{14}C]pyruvate, TPP, coenzyme A (CoASH), and either NADH or pyruvate as reducing systems leads to the formation of [^{14}C]acetyl-CoA. In this reaction the acetyl group of acetyl-TPP is partitioned by transfer to both CoASH (87 ± 2%) and water (13 ± 2%). When the E_1 component is incubated with 3-fluoro[1,2-^{14}C]pyruvate, TPP, and dihydrolipoamide, [^{14}C]acetyldihydrolipoamide is produced. The formation of [^{14}C]acetyldihydrolipoamide was examined as a function of dihydrolipoamide concentration (0.25–16 mM). A plot of the extent of acetyl group partitioning to dihydrolipoamide as a function of 1/[dihydrolipoamide] showed 95 ± 2% acetyl group transfer to dihydrolipoamide when dihydrolipoamide concentration was extrapolated to infinity. It is concluded that acetyl-TPP is chemically competent as an intermediate for the pyruvate dehydrogenase complex catalyzed oxidative decarboxylation of pyruvate.

The pyruvate dehydrogenase complex of *Escherichia coli* catalyzes the decarboxylation and dehydrogenation of pyruvate by the following sequence of reactions:[1]

$$H^+ + CH_3COCO_2^- + E_1\cdot TPP \rightarrow E_1\cdot HETPP + CO_2 \quad (1)$$

$$E_1\cdot HETPP + E_2\text{-lipoyl(S)}_2 \rightarrow E_1\cdot TPP + E_2\text{-lipoyl(SH)SCOCH}_3 \quad (2)$$

† This research was supported by Grant AM 28607 from the National Institute of Arthritis, Diabetes, and Digestive and Kidney Diseases.

0006-2960/86/0425-6036$01.50/0
